Sustainable Energy & Fuels

ROYAL SOCIETY OF CHEMISTRY

PAPER

View Article Online
View Journal | View Issue

Check for updates

Cite this: *Sustainable Energy Fuels*, 2024, **8**, 752

Open Access Article. Published on 15 2024. Downloaded on 16.08.24 13:28:08.
This article is licensed under a Creative Commons Attribution 3.0 Unported Licence.

Decentralised production of e-fuels for aviation: implications and trade-offs of a targeted small-scale production of sustainable aviation fuel based on Fischer–Tropsch synthesis

Andreas Meurer, * Patrick Jochem and Jürgen Kern

The introduction of Sustainable Aviation Fuel (SAF) is expected to play an important role in the decarbonisation of the aviation sector. Particularly for intercontinental flights, there is currently no near-term alternative to replacing fossil-based kerosene with sustainable liquid fuels. The current supply of conventional jet fuel is highly centralised through production at large-scale refineries. In light of future SAF production, there are also ongoing research activities and pilot projects focusing on small modular production technologies. This enables a decentralised fuel production, which could lead to a systemic shift in the current fuel supply infrastructure and value chains by enabling direct integration of renewable energy and fuel production in remote regions. To better understand the potential systemic role and relevance of such fuel production in the future energy system, we evaluate the process conditions and product costs of a decentralised Fischer–Tropsch based SAF production with maximised kerosene output as the only product of interest. The requirements for the product composition assumed in this study are particularly relevant and result in a reduced electrical plant efficiency of 35%. Compared to centralised production, the lower achievable electrical plant efficiency is compensated by a reduction of the indirect plant costs for modular units. The decentralised net production costs (NPC) of kerosene result in around 4.50 € per l in the baseline scenario, and between around 3.20 € per l and 6.15 € per l taking into account a variation of the assumptions. For a 2050 scenario, we evaluate NPC of 2.00 € per l, with a high confidence of ending up between 1.50 € per l and 2.75 € per l, considering the uncertainty assessment.

Received 4th September 2023
Accepted 8th December 2023

DOI: 10.1039/d3se01156a

rsc.li/sustainable-energy

1 Introduction

A significant reduction of greenhouse gas (GHG) emissions in the transport sector is necessary, to hold the increase in the global average temperature to well below 2 °C, as agreed in the Paris Agreement in 2015.[1] In 2018, with direct CO_2 emissions of more than 1 Gt[2] and under consideration of additional non-CO_2 effects, the aviation sector accounted for around 3.5% of the total anthropogenic effective radiative forcing.[2] An expected annual growth of the passenger and freight air traffic of around 3.5% in average over the next decades[3] will further increase the aviation sector emissions in the following years.[3] This places an additional burden on the long-term strategies and options that need to be implemented to reduce the emissions and climate impacts of the aviation sector.

A general framework for reducing GHG emissions, which was developed in the context of the transport sector, consists of three main pathways: Avoid, Shift, Improve.[4] While the most effective mitigation option after trip avoidance, a modal shift, can be applied to road transport in particular, this is much more complicated in the aviation sector due to missing alternatives for long distances. The growth in air traffic, especially in emerging economies catching up with the aviation capacity of established markets,[5] means that global aviation is unlikely to decline in the coming decades.[3] A feasible "shift" to more sustainable transport modes is possible for short distances, but around 80% of direct CO_2 emissions from aviation are caused by long-haul flights.[5] This impact is exacerbated by the greater non-CO_2 effects, which are amplified at the resulting higher flight altitude.[6] Significant reductions in GHG emissions must therefore mainly be achieved through the third pathway – improvement measures, which can be threefold.[3,7,8]

One pillar is efficiency improvements. An extensive list of possible tools includes *e.g.* improvements in aircraft fuel or payload efficiency, innovative ground taxiing concepts or adjustments to climb and descent, routing or flight altitude – accompanied by integrated digitisation of all these areas.[3,7,8] The second important option is the development of "zero-emission planes",[3] an aircraft technology that uses hydrogen

German Aerospace Center (DLR), Institute of Networked Energy Systems, Curiestr. 4, 70563 Stuttgart, Germany. E-mail: andreas.meurer@dlr.de; Tel: +49 711 6862 8100

This journal is © The Royal Society of Chemistry 2024

Open Access Article. Published on 15 2024. Downloaded on 16.08.24 13:28:08.
This article is licensed under a Creative Commons Attribution 3.0 Unported Licence.

combustion or electricity for the propulsion. However, the use of this technology is mainly foreseen for small aircraft and is likely to be limited to short-haul flights in the coming decades.[3,7] The third pillar is the introduction of sustainable aviation fuels (SAF), liquid kerosene-type fuels based on biomass or renewable electricity.[3,7] In most current projections, SAF is assumed to be the focus of improvement options and to account for the largest share of aviation emissions reductions over the next decades.[3,7,8] The envisaged important role of SAF is also being considered in legislation, such as the current proposal for the "ReFuelEU Aviation initiative"[9] as part of the European Union's (EU) "Fit for 55" package.[10] The proposal mandates minimum levels of SAF at EU airports, starting at 2% in 2025 and gradually increasing to 63% in 2050.[9] With minimum shares of 0.7% in 2030 and 28% in 2050, an additional sub quota is foreseen for the introduction of synthetic aviation fuels – renewable fuels of non biological origin (RFNBO) according the delegated regulation of the European Commission.[11] Under consideration of the requirements defined in ref. 12, RFNBO will mostly derive from renewable electricity as major energy carrier, so-called e-fuels (or power-fuels).[13]

The future role of e-fuels in aviation, including beyond the EU's or others statutory quota, is part of the current scientific debate. It will depend mainly on the techno-economic performance of the different technologies that can be used to produce SAF, the availability and costs of a supply of the required sustainable feedstocks and the possibilities of the infrastructural implementation. Numerous studies have assessed the plant efficiencies and the current and expected future costs of an electricity-based alternative fuel production. A comprehensive literature review was carried out by Ince *et al.*[14] to provide an overview of the literature relating to a systemic thermodynamic, techno-economic and life cycle assessment of different power-to-x pathways. König *et al.*[15] calculated the electrical efficiencies and current net production costs (NPC) of a Power-to-Liquid (PtL) process based on FT synthesis. Albrecht *et al.*[16] provide a standardised approach for the flow sheet simulation using the commercial Aspen Plus® and a subsequent techno-economic assessment using their in-house software tool TEPET. They report efficiencies and net production costs for Biomass-to-Liquid (BtL), Power-to-Liquid and Power-Biomass-to-Liquid (PBtL) processes for different plant production capacities between around 65 t/d and 250 t/d. They highlight the important role of the electricity price on the final production costs. This is also supported by the finding of Peters *et al.*,[17] which report efficiencies and product generation costs for a PtL process with integrated co-electrolysis for the synthesis gas production. The application of a co-electrolysis in a simplified plant setup is considered by Herz *et al.*,[18] who investigate achievable plant efficiencies and the economic feasibility with a focus on the production of chemicals. Adelung[19] carried out an extensive sensitivity and uncertainty analysis for a FT-based PtL process with external electrolysis, highlighting the relevance of the electrolysis operation strategy for the final product costs. A projection for production costs of jet fuel in the year 2050 is provided by Schmidt *et al.*,[20] which report literature-based efficiencies and production costs for Methanol- and FT-based pathways.

Common to all of the efficiencies and production costs reported in the above studies are the underlying assumptions of a centralised large-scale production and that the production costs relate to a wide range of products, including relevant amounts of carbon fractions other than those characteristic of kerosene.

However, there are new production routes that differ from conventional applications in terms of production capacity to "enable the implementation of new value chains".[20] Some of the current PtL demonstration projects are targeting small-scale applications[21] with a modular plant design for decentralised application, including and enabling a supply using only renewable electricity as the main energy source.[20] In addition to the ongoing development towards a certification of a 100% drop-in SAF,[22,23] a product certified for direct use in existing aircraft without the need for an additional conventional blending component, an ASTM task force is also working on 100% non-drop-in SAF standards,[23] which could be particularly relevant for decentralised applications.

In the medium to long term, a decentralised production strategy in combination with a certified 100% SAF product could be particularly suitable for an on-site production of SAF directly at the airport. Especially for remote airports with currently long and extensive transport distances to the next refineries, such production can be beneficial. This study provides the basis for a systematic evaluation of the possible future role of a decentralised modular production of SAF. A newly developed open-source capable Python-based modelling framework is used to investigate the production process based on a generic method chain and to answer the following research questions, which have not been addressed by the existing research described above:

- What are the most relevant process steps and what are the efficiency trade-offs of a modular small-scale PtL plant with explicit consideration of boundary conditions relevant for decentralised SAF production from a systemic perspective?
- What are expectable net production costs of a modular small-scale production of SAF in a baseline scenario and a projection for 2050 under consideration of the constraints relevant for a decentralised PtL production?

The method chain presented in this study can also serve as a blueprint for the comprehensive assessment of other process setups in the context of synthetic fuel production. The study further identifies necessary research areas, which are particularly relevant for the decentralised production of 100% drop-in SAF production.

This paper is structured as follows: Section 2 provides information on the process setup, constraints and the general methodology. This is followed by the presentation and discussion of the results in Section 3, focussing on a detailed analysis of the different process steps and operation parameters in Section 3.1, the assessment of achievable plant efficiencies in Section 3.2 and the expectable net production costs of kerosene in Section 3.4. Section 4 concludes the key findings, highlights

Open Access Article. Published on 15 2024. Downloaded on 16.08.24 13:28:08.
This article is licensed under a Creative Commons Attribution 3.0 Unported Licence.

open research areas and gives an outlook on possible follow-up studies.

2 Methods

The process design evaluated in this study (*cf.* Fig. 1), which considers a decentralised implementation approach and a modular unit design, is described in Section 2.1. For the subsequent calculation and analysis of the process, a Python-based modular chemical process model is developed and applied, which is further elaborated in Section 2.2. The parameter sampling and process optimization under consideration of the underlying constraints and assumptions is shown in Section 2.3 and 2.4. The methodology and assumptions of the techno-economic assessment are part of Section 2.5.

2.1 Process design

Following the approach of decentralised kerosene production, we assume that certain boundary conditions are particularly relevant. Those can be summarised to the necessity of a reliable feedstock supply of constant quantity and quality with a low regional impact as well as a low plant complexity and thus the possibility of a smooth plant operation.[24] Since the supply of renewable electricity is technically possible at any location (poor RE potentials have an impact on electricity supply costs, but not on the overall technical feasibility), a power-to-liquid process is considered a reasonable technology for this application.

In this study, high temperature co-electrolysis (co-SOEC) is selected for synthesis gas production, as this technology is envisaged to be part of a currently planned commercial PtL production plant.[25] As during co-SOEC, CO_2 and H_2O is directly converted into the required syngas components H_2 and CO in one single process step, it is particularly suitable for a modular approach, reducing the amount of required process steps. A Fischer–Tropsch (FT) reactor is chosen for the synthesis, as it is a typical synthesis type of modular units which are currently under development[26] or already in operation.[27] Syncrude from FT synthesis is also particularly suitable for kerosene production, as it requires less refining effort than other synthesis technologies.[28] The product separation consists of two condensation stages, as shown in Fig. 2, which corresponds to the approach of low plant complexity and is generally in line with the process setup of small-scaled modular units.[21,29] The process is further explained in Section 2.2. In order to increase the kerosene yield and the required proportion of isomerised paraffins, a hydrocracker (HC) is considered as part of the process. In contrast to current research that examines a combination of FT and HC in a single reactor,[30] this study considers the HC as a separate process step.

The authors recognise the need for and the benefits of a highly detailed process simulation. However, this study is primarily concerned with technology insights, impacts and conclusions that have a systematic impact on the technology as part of the overall energy system. The process design to be evaluated is, therefore, simplified and reduced to those components that are expected to be either highly relevant to the final product composition (leading to implications for the infrastructural embedding in the system) or to have a significant impact on production costs. Additional equipment is thus not part of the technical process evaluation and is considered *via* additional cost factors in the techno-economic assessment. This approach is carried through to the modelling of individual process steps, which vary in detail according to their relevance and impact on the process efficiency, cost and product composition.

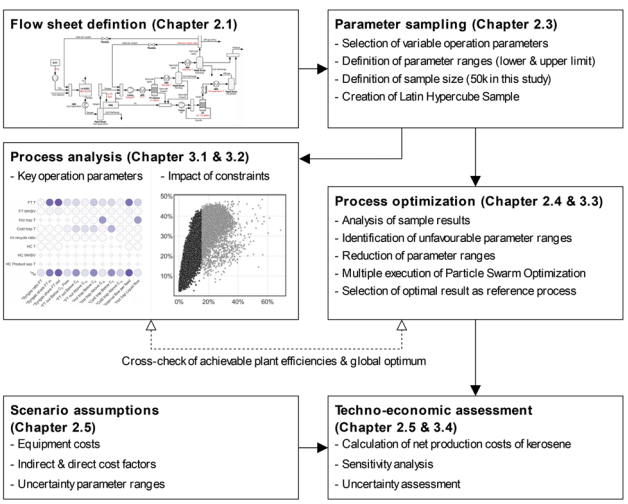

Fig. 1 Method chain overview.

2.2 Process model

A Python-based modular process framework is developed to iteratively compute a steady state process condition. The process state is considered stable if the specific deviation of both mass flow and flow composition is less than 0.05%. For all calculations, real gas behaviour is considered, according to which the Peng–Robinson equation of state[31] with the Boston–Mathias alpha function is used in the model. In addition to the feed gas and syngas components H_2O, CO_2, H_2 and CO, linear paraffins (*n*-paraffins) and branched (isomerised) paraffins (iso-paraffins) up to a carbon chain length of C_{45} are considered in the model. Physical and thermophysical properties of the hydrocarbons are derived on the basis of Yaws.[32–34] To account for the many different isomers, an artificial representative iso-paraffin is determined for each carbon chain length, whose properties are calculated from the average values of the iso-paraffins with up to two branches.

2.2.1 Direct air capture. To be independent of site-specific conditions, we consider a Direct Air Capture (DAC) unit to provide CO_2. The CO_2 supply is considered external from the synthesis process and does not directly affect the process operation. It is therefore modelled with a low level of detail, only considering an electrical energy demand of 250 kW h_{el} per t_{CO_2} (ref. 35) and a thermal energy demand of 1750 kW h_{th} per t_{CO_2} (ref. 35) for the baseline scenario. For the 2050 projection, an electricity demand of around 180 kW h_{el} per t_{CO_2} and thermal energy demand of around 1100 kW h_{th} per t_{CO_2} is considered.[35]

 This journal is © The Royal Society of Chemistry 2024

Open Access Article. Published on 15 2024. Downloaded on 16.08.24 13:28:08.
This article is licensed under a Creative Commons Attribution 3.0 Unported Licence.

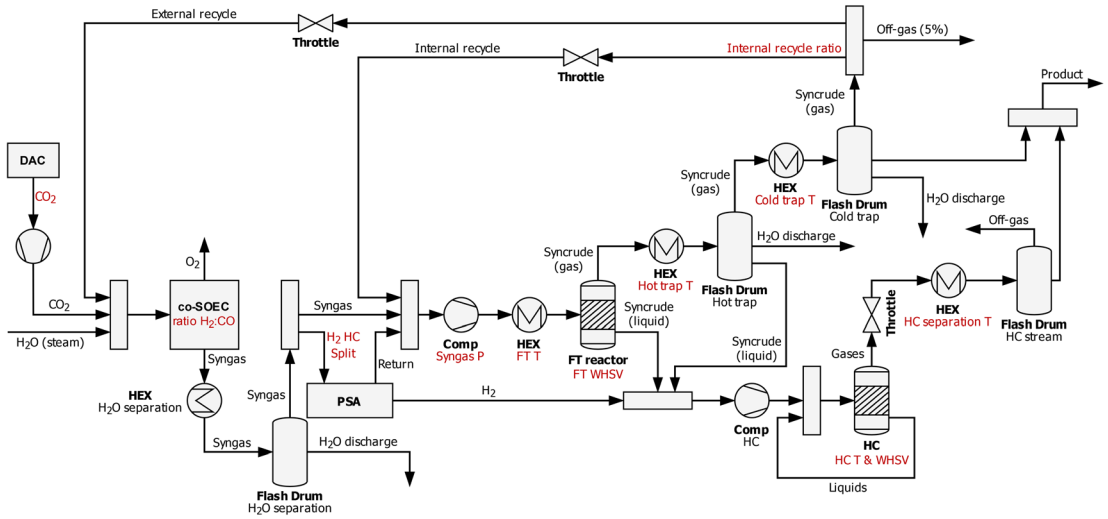

Fig. 2 Simplified process flow sheet of the PtL production evaluated in this study. Operation parameters which are varied during the process analysis described in this study are highlighted in red.

2.2.2 co-SOEC. The co-SOEC unit converts CO_2 and water steam into the syngas, a mixture of H_2 and CO. As to the authors' knowledge, there is currently no reactor model in the literature that is suitable for the simplified and generic approach considered here, the co-SOEC is modelled on the basis of the technical data sheet of the SynLink SOEC unit from Sunfire,[36] which is also being considered as part of the norsk e-fuel PtL plant.[25] The CO_2 conversion rate is fixed to 80% and the reaction temperature is set to 850 °C. The H_2 to CO ratio of the outgoing syngas stream is considered a variable operation parameter and determines the H_2O conversion rate, the syngas stream composition and the flow rate of the O_2 stream which leaves the co-SOEC unit separately. Further components which are part of the feed stream to the co-SOEC unit due to the admixture of the external recycle stream are considered to be not affected by the co-SOEC. The electrical energy demand is calculated on the basis of the lower heating value (LHV) of the syngas produced and the electrical efficiency of 80%, which is derived from the efficiency of an SOEC[37] as a proxy for the co-SOEC. This efficiency is in line with the one reported by Sunfire.[36] An efficiency gain of 5% is considered for the 2050 scenario based on the data reported by Smolinka *et al.*[37]

2.2.3 Fischer–Tropsch synthesis. The FT synthesis – converting the syngas components H_2 and CO into hydrocarbon chains of different species and chain lengths – is modelled as a kinetic reactor using the kinetic parameters according to Sun[38] and Loewert *et al.*,[29] which is affected by the syngas composition, the temperature (T), pressure (P) and weight hourly space velocity (WHSV). Their model is a further development based on the kinetic reactor model of Kwack *et al.*[39] and has been specifically designed for a microstructured FT reactor, which is considered to be a suitable reactor technology for small-scale, decentralised applications. The reactor model considers exclusively the formation of *n*-paraffins as hydrocarbon species which is in line with the qualitative description of cobalt-catalysed low temperature FT synthesis (LTFT), leading to a highly paraffinic syncrude composition with only minor shares of aromatics and unsaturated or oxygenated hydrocarbons.[40] The resulting mass fraction distribution generally follows the Anderson–Schulz–Flory model, but considers an increase in methane selectivity which can be observed in practice.[41]

2.2.4 Hydrocracking. Hydrocracking is a catalytic process with the focus on the cracking of long-chained hydrocarbons into shorter fractions. It is accompanied by an isomerisation, the removal of heteroatoms like oxygen, sulphur or nitrogen and the reduction of the aromatic content and is especially suitable for the refining of cobalt-based LTFT syncrude.[28] The Langmuir–Hinshelwood–Hougen–Watson kinetic reactor model from Pellegrini *et al.*[42] is implemented. It is designed on the basis of a LTFT syncrude output and comprises specific reaction rates for the isomerisation of linear paraffins and cracking of iso-paraffins up to chain length of 70 carbon atoms. To account for the difference in the maximal considered carbon number of C_{45} in this study, the adsorption coefficient is calculated with the lumped fractions above C_{30} based on Selvatico *et al.*[43] The vapour and liquid shares of each fraction are summed up, as the kinetic equations are the same for both fractions.[42] As a simplification, this model does not consider a breakage distribution function but assumes a breaking in the middle of the isomerised hydrocarbon chains.[42]

2.2.5 Pressure swing adsorption. The hydrocracking unit requires an additional feed stream of hydrogen, which is considered to be separated from the syngas stream to the FT reactor using a Pressure Swing Adsorption (PSA). The PSA is considered a common process in the petrochemical industry for hydrogen purification.[44] As it is generally possible to provide a high purity hydrogen stream for different pressures, temperatures and feed compositions,[44] the PSA in this study is modelled at a low level of detail. Since the operating parameters are within the temperature and pressure ranges reported by Sircar and Golden,[44] a separation of H_2 with a recovery rate of 80% is modelled without further consideration of the feed gas composition.

Open Access Article. Published on 15 2024. Downloaded on 16.08.24 13:28:08.
This article is licensed under a Creative Commons Attribution 3.0 Unported Licence.

2.2.6 Process and product constraints. We define several major constraints related to process operation and product output composition that must be met. Two process-related constraints apply to the gas composition at the FT reactor. To enable a uniform reaction throughout the reactor and improve the catalyst stability, it is favourable that the syngas H_2 to CO feed ratio of the reactor is close to the usage ratio during the synthesis.[41] The H_2 to CO syngas ratio is therefore limited to a range of 1.9 and 2.3, which corresponds to a deviation of around $\pm$10% of the H_2 to CO usage ratio of around 2.1, which is typical for cobalt-based LTFT reaction. The second constraint limits the minimum share of H_2 and CO in the reactor outlet stream. According to Tucker *et al.*,[45] a minimum molar syngas share of 15% should be maintained at the reactor outlet to avoid a significant irreversible catalyst deactivation. The last process-related restriction addresses the decentralised operation. Self-sufficiency does not only comprise to the supply of electrical but also of thermal energy. The thermal energy which can be provided by combustion of the off-gases (based on the lower heating value) therefore has to cover the thermal heating demand at high temperatures. A simplified heat integration using pinch point analysis (PPA) is implemented to calculate the required leftover heating demand. This takes into account all thermal energy flows due to temperature adjustments, phase changes such as in flash drums or the FT reactor, and the chemical reaction enthalpies in the reactors, including the highly exothermic FT reaction. Based on the composite curves of all hot and cold streams on their respective temperature levels, the hot utility is calculated. However, for simplification, we have not included the additional cost of the required heat integration network.

Two major constraints are further defined for the product composition. The shares of hydrocarbon fractions below and above the characteristic kerosene range, which is considered between C_8 and C_{16} in this study,[46] are limited to a maximum of 15 mass% each. Those constraints are considered a simplified approach to introduce a product-related limitation. Current regulations for fuel specification mainly define fuel properties, but do not give explicit guidelines for the fuel composition. This applies to both conventional Jet A-1 (ref. 47) and also currently approved SAF pathways.[48] The interrelation between fuel composition and resulting properties is highly complex[49] and beyond the scope of this work. The fuel property assessment in combination with a process optimisation and evaluation is highlighted as one major open research area in the following course of this study.

2.2.7 Process efficiency. In this study, we use the electrical plant efficiency η_{el} to evaluate the process. The useable energy content is calculated based on the mass flow $\dot{m}$ and the LHV of the outgoing product stream. The electrical energy demand P is induced by the DAC, the co-SOEC and the sum of the compressors, resulting in the calculation of electrical efficiency according eqn (1):

$$\eta_{el} = \frac{\dot{m}_{product} LHV_{product}}{P_{DAC} + P_{co\text{-}SOEC} + P_{compressors}} \quad (1)$$

2.3 Parameter sampling

A Latin Hypercube Sampling (LHS) is used to generate a set of 50 000 parameter combinations, taking into account a variation of the twelve operation parameters listed in Table 1 within the defined ranges. The LHS is a method for a quasi random sampling of parameter values. We use LHS as it ensures a uniform distribution over the selected parameter ranges and is considered a favourable method over a simple random sampling.[50] Based on the parameter sample, a steady state process is calculated for each parameter combination. The reasons for conducting such extensive number of calculations are threefold:

1. The analysis of the calculation results under varying operation parameters provides insights on the process operation and expected effects on efficiency and product composition. The most relevant process parameters with a major impact on the process performance indicators can be identified.

2. In order to reduce the computational effort for the subsequent execution of the Particle Swarm Optimisation (PSO), operating parameters are determined that lead to process parameters that do not correspond to the technical process constraints defined in Section 2.2.6. The identified parameter ranges are excluded for the following process optimization calculation and thus reduce the size of the search space.

3. The broad exploration of the parameter space enables the identification of parameter regions with local maxima.

2.4 Process optimisation

We selected the PSO as optimization algorithm for the maximisation of the electrical process efficiency. As the PSO is a global non-linear optimisation method and is characterised by a fast convergence rate and effective implementation in modelling environments,[51] it is particularly suitable for the process setup and modelling approach in this study.

During the optimisation, any calculation that violates the constraints defined in the previous sections is excluded from the optimisation process. To account for the fact, that a global optimisation using a metaheuristic approach such as PSO cannot ensure that the global optimal solution is found,[52] several measures are taken to increase the reliability of the PSO results.

Table 1 Operation parameters and value ranges of the Latin Hypercube Sampling

Parameter	Units	Lower limit	Upper limit
Feed ratio $CO_2 : H_2O$	—	0.7	1.3
co-SOEC ratio $H_2 : CO$	—	2.0	2.5
H_2 HC split	%	3.0	15.0
Syngas P	MPa	1.5	3.0
FT T	K	480	513
FT WHSV	g h^{-1} $g_{catalyst}^{-1}$	1.0	5.0
Hot trap T	K	400	465
Cold trap T	K	280	380
Int recycle ratio	%	80.0	98.0
HC T	K	600	645
HC WHSV	g h^{-1} $g_{catalyst}^{-1}$	1.0	5.0
HC separation T	K	350	450

This journal is © The Royal Society of Chemistry 2024

Open Access Article. Published on 15 2024. Downloaded on 16.08.24 13:28:08.
This article is licensed under a Creative Commons Attribution 3.0 Unported Licence.

1. Four different PSO runs with varying setting parameters are carried out. A number of 72 particles is selected for all four runs, limited due to infrastructural boundary conditions of the computational cluster used but complying to Piotrowski *et al.*,[53] which conclude the best results within a swarm size of 70 to 500 particles for complex problems with the PSO method considered here.

2. The resulting maximised efficiencies are adjusted for the underlying additional constraints individual to this study and compared with expectable plant efficiencies based on the current literature.

3. The PSO results are cross-checked with the calculated plant efficiencies based on the LHS to identify, if possible parameter ranges leading to further increased efficiencies remained undetected by the PSO.

The maximisation of the electrical plant efficiency is chosen as optimisation criterion for the PSO because it is subject to less uncertainty than the calculation of the net production costs of kerosene (NPC). We assess this approach as sufficiently accurate and also representative for production cost optimisation, as there is a direct correlation between plant efficiency and production costs, as demonstrated in the remainder of this study.

2.5 Techno-economic assessment

Using the equipment dimensions resulting from the steady-state process, the required input commodities and the outgoing product stream, the NPC of two scenarios are calculated based on Peters *et al.*[54] For both scenarios, we perform a sensitivity analysis and the assessment of the distribution of resulting NPC, considering the uncertainty of the input parameters based on a probability sample.

2.5.1 Equipment cost estimation. For the estimation of the capital expenditures (CAPEX) for the plant equipment, we employ generic cost functions for the different component types based on Peters *et al.*[54] For the CAPEX estimation, the FT reactor and Hydrocracker are equated with multi tubular heat exchangers. The underlying cost assumptions of Peters *et al.*[54] which refer to 2002 are converted to €$_{2019}$ using the average 2019 USD exchange rate and the Chemical Engineering Plant Cost Index (CEPCI). For the special core components which cannot be easily abstracted with common equipment – that applies to the co-SOEC and the DAC – we use the literature-based values shown in Table 2.

Table 2 Cost assumptions for non-generic components

Component	Units	$CAPEX_{baseline}$	$CAPEX_{2050}$
DAC[35]	€ per t_{CO_2} a^{-1}	730	199
co-SOEC[37]	€ per Nm^3 per h	8800	1050
Commodity	**Units**	**$Cost_{baseline}$**	**$Cost_{2050}$**
Electrical energy	€ per kW h	0.10	0.05
Process steam[16]	€ per t	26.3	26.3
Waste water[16]	€ per m^3	2.5	2.5

To complete the estimation of total required capital investment, additional plant expenses which are typical for fluid processing plants are considered as a percentage of the delivered equipment costs.[54] Some of the major economic advantages of a modular small-scale plant setup can be accounted to savings in cost categories which are covered by those CAPEX-factors. To the authors knowledge, no detailed information on the additional capital investment items for modular pre-fabricated plants can be found in current literature. Therefore, we define various assumptions which are described in Table 3, showing all direct and indirect additional cost-factors. The specific commodity and utility costs relevant for the calculation of the direct operational expenses are provided in Table 2.

2.5.1.1 Net production costs of kerosene. Eqn (2) summarizes the general calculation of the net production costs for a litre of product output:

$$\mathrm{NPC} = \frac{\mathrm{FCI}\dfrac{i(1+i)^n}{(1+i)^n-1} + i\mathrm{WC} + \sum_{\mathrm{DO}} f_{\mathrm{DO}}\mathrm{RP}_{\mathrm{DO}} + \sum_{\mathrm{Cm}} \dot{m}_{\mathrm{Cm}} c_{\mathrm{Cm}}}{\dot{m}_{\mathrm{product}}} \quad (2)$$

with i as interest rate, n as plant lifetime, WC as working capital, DO as direct OPEX items, f as factor for the operational expenditures (OPEX), RP as OPEX reference parameter, Cm as commodities, $\dot{m}$ as yearly mass flow and c as specific commodity cost. It takes into account the annual capital costs for the fixed capital investment (FCI) on the basis of the annuity method with the economic assumptions based on Table 2 and the generic equipment cost estimation according.[54] In addition, the interest of the working capital, the operational expenses according Table 3 and the expenses for commodities and utilities, which are based on the specific costs according Table 2 and the respective yearly demand, are considered. All costs refer to a plant with a production capacity of 10 000 l per day, as exemplary fuel consumption for a medium-sized remote airport, a lifetime of 20 years and full load hours of 8000 hours per year. We assume that there is no monetary valorisation of by-products such as oxygen or light hydrocarbons. The NPC do not cover any additional downstream fuel handling costs or duties.

2.5.1.2 Sensitivity and uncertainty analysis. We perform a sensitivity analysis, varying commodity costs, plant capacity, CAPEX and OPEX factors in a range of ±80% and a step size of 10%.

In order to evaluate the impacts on the NPC due to the likely deviation of the underlying input parameters compared to the underlying scenarios, we perform an uncertainty assessment. With the assumptions of the base scenarios as the reference point, we create a sample of 10 000 input parameter combinations with a triangular probability distribution with the ranges defined in Table 4.

The range of the equipment which is generically calculated according Peters *et al.*[54] derives from the capital cost estimation accuracy of ±30%.[54] For the other core components, a range of ±50% is assumed as these are still relatively new technologies for which an estimate of the costs may be subject to greater

Open Access Article. Published on 15 2024. Downloaded on 16.08.24 13:28:08.
This article is licensed under a Creative Commons Attribution 3.0 Unported Licence.

Table 3 Ratio factors of additional CAPEX and OPEX to the equipment cost

Item	Reference parameter	Peters *et al.*[54]	Own assumption
Direct CAPEX			
Equipment installation	Equipment cost	47%	47%
Instrumentation & control	Equipment cost	36%	36%
Piping	Equipment cost	68%	68%
Electrical installations	Equipment cost	11%	11%
Buildings	Equipment cost	18%	5%[a]
Yard improvements	Equipment cost	10%	5%[b]
Service facilities	Equipment cost	70%	10%[c]
Indirect CAPEX			
Engineering & supervision	Equipment cost	33%	10%[d]
Construction	Equipment cost	41%	10%[e]
Legal expenses	Equipment cost	4%	4%
Contractors fee	Equipment cost	22%	22%
Contingency	Equipment cost	44%	0%[f]
Direct OPEX			
Operating labour			41 € per h[g]
Operating supervision	Operating labour	15%	0%[h]
Maintenance & repairs	FCI	4%	4%
Operating supplies	Maintenance and repairs	15%	15%
Laboratory charges	Operating labour	15%	0%[j]
Taxes	FCI	0%	0%
Insurance	FCI	1%	1%
Working capital	FCI	15%	15%

[a] For a modularised system design where all main components are provided in containers, it is assumed that an extensive additional building erection is not necessary. Therefore the CAPEX factor is reduced. [b] Analogous to the buildings, it is assumed that without an extensive additional building erection substantial yard improvement is not necessary. [c] One intended major advantage of a modularised and decentralised system design is the significant reduction of operation and maintenance activities. Thus, it is assumed that consequently also the necessity and the extent of service facilities is significantly reduced. [d] In the scenario of a decentralised and modularised system design, the engineering of the plant design is highly facilitated as it is no longer a completely individual plant design. Therefore, a relevant decrease of the CAPEX factor is assumed. [e] Due to the modularised scenario which might lead to a significant increase in the efficiency of pre-assembly of the process steps, a significant reduction of the construction costs is assumed. [f] Due to possible pre-fabrication, no contingency considered. [g] Concerning the decentralised approach, which comes with a highly facilitated plant operation, the above estimation method is assumed to be not expedient. As the plant operation is considered highly automated, in the following assessment 16 employee-hours per day are assumed, being representative for two 8 hour shifts. The hourly wage is based on.[55] [h] It is assumed, that for a decentralised production with minor number of employees and a highly automated process operation, no operating supervision is necessary. [j] Following the scenario of a highly automated process operation using modular process units for the operation at a predefined operation point and product composition, laboratory charges are assumed to be negligible.

Table 4 Uncertainty parameter ranges

Category	Range
Generic equipment	±30%
Non-generic core components	±50%
CAPEX factors	±30%
CAPEX factors adjusted	±50%
OPEX factors	±30%
OPEX factors adjusted	±50%
Operating labour	±50%
Commodities	±50%
Plant efficiency	±25%

fluctuations. The FT reactor is subject to the same considerations, resulting in a ±50% uncertainty range also being applied. To account for the additional uncertainty of our own assumptions regarding the cost-factors, the uncertainty range of the adjusted CAPEX and OPEX factors is also increased to ±50%.

3 Results and discussion

This section is divided into three parts. In the first, we show and discuss the impacts of the operation parameters on the plant performance. In the second part, we addresses the identification of an optimised process operation point with high electrical efficiency, which forms the basis for the third part which deals with the techno-economic assessment of the selected process setup. For ease of reference, all plant performance indicators are indicated by asterisks in the following figures (*e.g.* *syngas ratio FT). The values describing the operating parameters remain unmarked. The underlying data of all following results is provided on zenodo.[56]

3.1 Process analysis

Of the set of 50 000 samples, around 44 000 calculations converged to a steady-state process and form the basis for the following analysis. The maximum electrical efficiency of the plant, without considering product composition constraints, is

 This journal is © The Royal Society of Chemistry 2024

Open Access Article. Published on 15 2024. Downloaded on 16.08.24 13:28:08.
This article is licensed under a Creative Commons Attribution 3.0 Unported Licence.

around 48%, which is in line with current literature, *e.g.* König *et al.*,[15] Albrecht *et al.*[16] or Schmidt *et al.*[20]

Fig. 3 shows the correlation between the varying input operation parameters and selected performance indicators of the process. Only few operation parameters show a systematic impact on the plant performance and process operation states. With a coefficient of determination (R^2) of around 0.65, the FT reactor temperature is the operation parameter that has the most decisive individual impact on the electrical process efficiency. Apart from the FT reactor space velocity, which also shows a tendency to systematically influence the plant efficiency ($R^2 \approx 0.1$), no other systematically decisive parameters with respect to the electrical efficiency can be identified.

Also with regard to the other operation states tracked, significant systematic influences can be seen primarily in the FT reactor temperature. This is mainly due to its effect on the composition of the outgoing gas stream, which is twofold. An increase in reaction temperature leads to an increased reactor activity – equivalent to an increase in the conversion rate of the synthesis gas. When there are fewer syngas components in the effluent stream, less gas needs to be recirculated through the internal and external gas recirculation streams because most of the converted syngas is separated in the hot and cold trap. As the flue gas flow is fixed at 5% of the recycle flow, increasing the recycle flow increases the absolute losses of energy intensive syngas components and CO_2. This is the same reason, why a low space velocity (WHSV) tends to lead to higher efficiencies, as at lower WHSV, the syngas conversion rate in the reactor is increased. The relationship between the process-internal flow and the achievable electrical efficiencies is shown in Fig. 4.

The second effect of FT reactor temperature on gas stream composition is its influence on the chain growth of the hydrocarbons during synthesis. Increasing reaction temperatures reduce the growth probability and thus result in a hydrocarbon output that is in average shifted towards shorter chain lengths. In addition to the recirculation stream, this

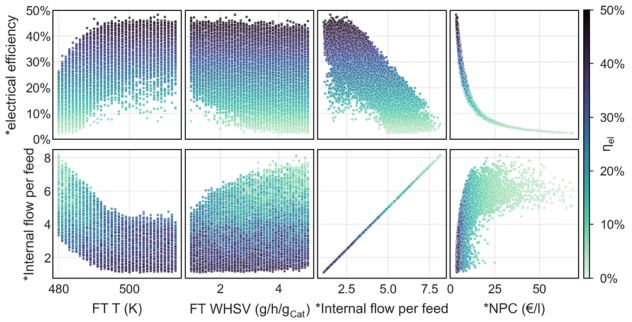

Fig. 4 Relationship between key operation parameters and selected plant indicators. The NPC refer to the baseline cost scenario.

subsequently affects the proportions of hydrocarbon fractions condensing in the hot and cold traps and thus the final product composition. However, the reactor temperature mainly affects the proportions of product types consisting of heavier fractions (*e.g.* waxes or diesel) and shorter fractions (*e.g.* naphtha or gasoline). The proportion of kerosene is not significantly affected, since the maximum of the parabolic distribution of chain lengths, which is in principle typical for an FT reactor,[41] always lies within the kerosene fraction in the reaction temperature range considered.

The process operation parameters with the most systematic effect on the kerosene fraction of the product stream are the hot trap and cold trap temperatures. The hot trap temperature controls the separation of the longer hydrocarbon chains and leads to an increase in long chain hydrocarbons and therefore a decrease in the specific share of kerosene fraction with increasing temperature. The separation of the shorter hydrocarbon fractions is mainly controlled by the cold trap temperature. Lowering the temperature results in a broader product spectrum and increased product yield, but a decrease in the specific proportion of kerosene fraction hydrocarbons.

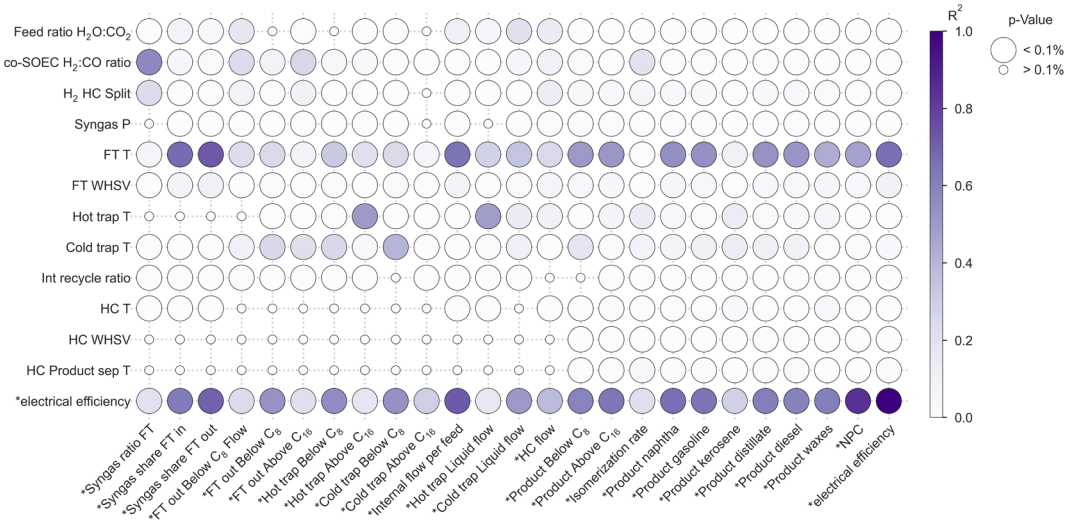

Fig. 3 Correlation matrix showing the coefficient of determination (R^2) and the statistical significance based on the p-value for 43 959 samples. Due to the large sample size, a p-value of <0.001 (0.1%) is chosen as the criterion for statistical significance.

Open Access Article. Published on 15 2024. Downloaded on 16.08.24 13:28:08.
This article is licensed under a Creative Commons Attribution 3.0 Unported Licence.

Although the syngas ratio provided by the co-electrolysis unit also has a systematic effect on some operating states, *e.g.* the isomerisation rate, it cannot be chosen arbitrarily, but is limited by the requirements of the feed gas composition entering the FT reactor. Those process-related and additional product-related constraints and their impacts on process efficiency are discussed in the following section.

3.2 Plant efficiencies under process and product constraints

Fig. 5 shows the effects of the process constraints in the FT reactor and the assumed product composition constraints. These effects are shown both for the achievable plant efficiency and for selected operating condition parameters. The data used for this graph is derived from all sampling results that have achieved a steady state.

Although filtering by the constraints assumed for the FT reactor excludes more than 60% of the calculation samples, it results in only a small reduction in achievable plant efficiencies. Without consideration of further constraints, the highest efficiencies result at around 45%, which is in line with current literature on overall process efficiencies without restrictions on the product composition.[15,16,57] For the constraints associated with the FT reactor, no further systematic constraints on other operating states, or conclusions on operating parameters, can be drawn.

The restriction of the long-chained product fractions above C_{16} to a maximum of 15 mass% excludes another more than 25% of the original samples, but has no general effect on the highest achievable efficiency. A notable impact can mainly be observed for the internal flow, where the upper around 25% are excluded. This is in line with the observations made in Section 3.1, as a higher proportion of long-chained hydrocarbons in the product output is generally favoured by low reactor temperatures, which are generally associated with an increase in internal flow.

Adding the final constraint, the limitation to a maximum share of 15 mass% of the short product fractions below C_8, excludes another 10% of the sample. This results in a total leftover of only around 1.5% of the initial sample size if all constraints are considered and excluded (626 from 43 959 samples). This constraint has the highest effect on the achievable efficiencies, reducing the maximum value to a total electrical plant efficiency of around 35%. An explanation consistent with the relationships described in Section 3.1 is again found in the reactor temperature as the most decisive parameter. High plant efficiencies are generally enabled and promoted by increasing reactor temperatures. In contrast to the long-chain fractions, an increase in the FT reactor temperature for the short-chain hydrocarbons results in an increase in their proportion of the product output. Reducing their share on the final product is therefore generally associated with a reduction in achievable plant efficiencies for the plant configuration considered here. Unlike the previous constraints, this constraint allows us to restrict the operating parameter range for the following optimisation, where the upper temperature range of the hot trap can be neglected as it is unlikely to provide a product composition within the defined constraints.

The importance of the constraints, especially those related to the product composition, are further highlighted by Fig. 6, which shows the relation between the constrained parameters

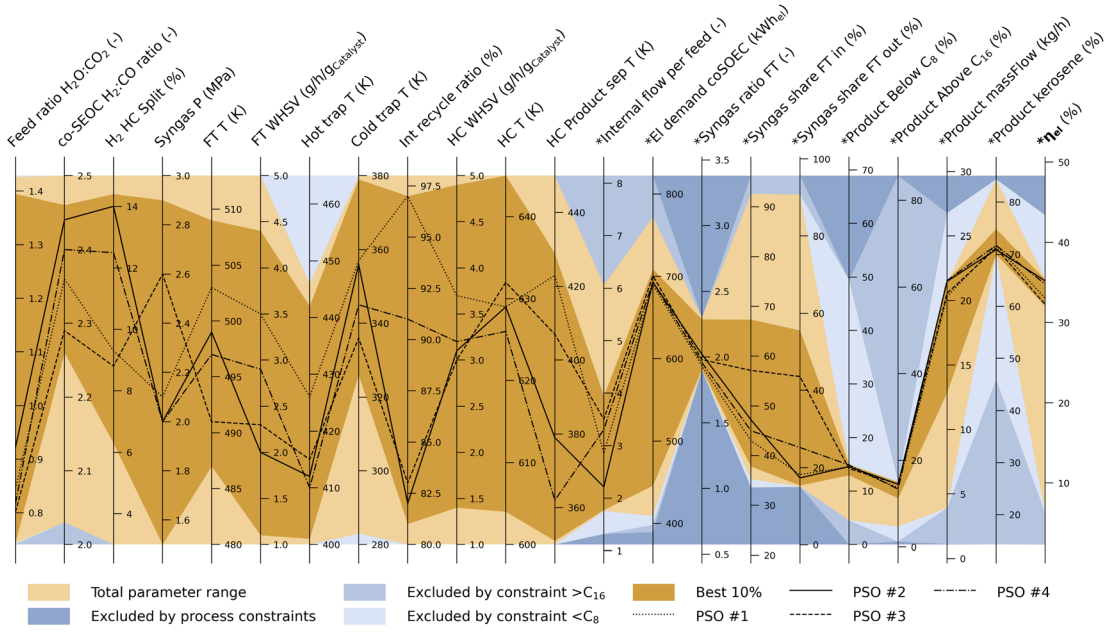

Fig. 5 Parallel coordinate plot showing the range of operation parameters according to Table 1 and the resulting range of the performance indicators on the vertical axes for all LHS and PSO calculation runs. The electrical efficiency is shown on the right. Blue shaded areas show the gradual exclusion of parameter ranges due to process- and product-related constraints. The dark orange area shows the parameter ranges that result in the top 10% of electrical efficiency from all calculations meeting all constraints. The lines show the optimal solution from each PSO run, with the solid line representing the absolute maximum and reference process selected for the techno-economic assessment.

 This journal is © The Royal Society of Chemistry 2024

Open Access Article. Published on 15 2024. Downloaded on 16.08.24 13:28:08.
This article is licensed under a Creative Commons Attribution 3.0 Unported Licence.

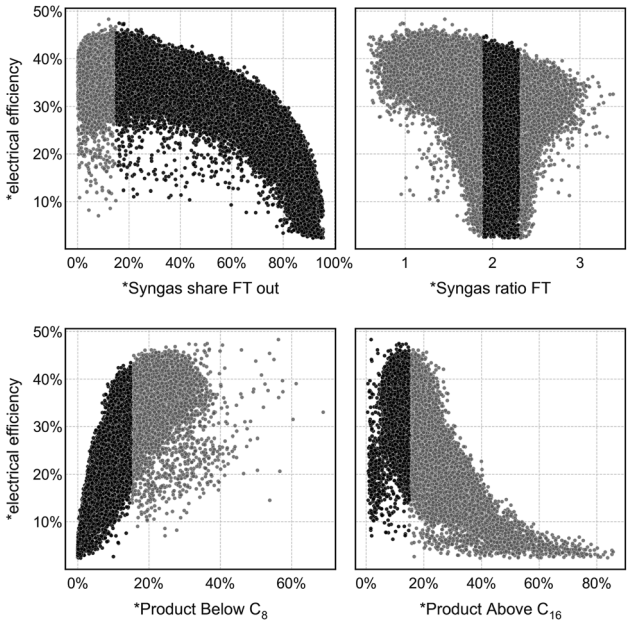

Fig. 6 Relationship between the four constrained process state parameters described in Section 2.2.6 and the achieved electrical efficiencies of all samples. Results that do not meet the constraints assumed in this study are displayed in grey. The resulting Pareto frontiers allow an assessment of the trade-offs in terms of electrical efficiency if the constraints are further narrowed.

and electrical efficiencies of all samples. Whereas the limits of the process constraints do not have a substantial impact on achievable efficiencies, especially the limit on the amount of short-chain hydrocarbons does have a considerable impact on efficiency. Starting from a share of 20 mass% of hydrocarbons below C_8, any reduction of this constraint results in a steep decline in achievable efficiencies. A similar trend, albeit to a lesser extent, can also be seen when the share of long-chain hydrocarbons is restricted. Nevertheless, low amounts of long-chain product fractions do not necessarily preclude achieving high efficiencies.

The strong impact of the introduced product-related constraints on process efficiencies underlines the future need for further detailed analysis of the product composition requirements that need to be met to enable use as a near drop-in fuel in the context of decentralised applications. With a better understanding of the requirements, an increase in plant complexity, *e.g.* through more extensive product separation, can then be evaluated in terms of its overall impact (on efficiency, costs and product composition).

3.3 Optimisation and process selection

The four PSO runs yield maximal electrical efficiencies between 33% and 36%, which is in line with the maximal efficiencies derived by the LHS discussed in the previous section. The operation parameters resulting in the maximal efficiencies for each PSO run are shown in Fig. 5. They support the results from the previous section, that high plant efficiencies under consideration of the constraints are generally achievable *via* a broad spectrum of possible operation parameters. A review based on the top 10% of achievable efficiencies of all calculations, also shown in Fig. 5, leads to the conclusion that the narrow clustering at different operating parameters (such as HC T) of the optimal solutions of the four PSO runs is not systematic. For the following techno-economic assessment, the best result from PSO#2 is selected and used as reference process.

3.4 Net production costs of kerosene

Based on the operating point selected in the previous section, the NPC are presented below and a sensitivity and uncertainty analysis is carried out. Using the assumptions described in Section 2.5, the net specific production costs are around 4.50 € per l in the baseline scenario and around 2.00 € per l in the projection for 2050. The breakdown of the cost components is shown in Fig. 7. In both scenarios, the production costs are dominated by the operational expenses, with around 70% in the baseline scenario and around 75% in the 2050 scenario. Although absolute production costs are substantially reduced in the projection for 2050, the overall distribution of costs is not significantly different between the two scenarios. At over 50% in both scenarios, the cost of electricity supply is the single cost component with the highest share on the NPC.

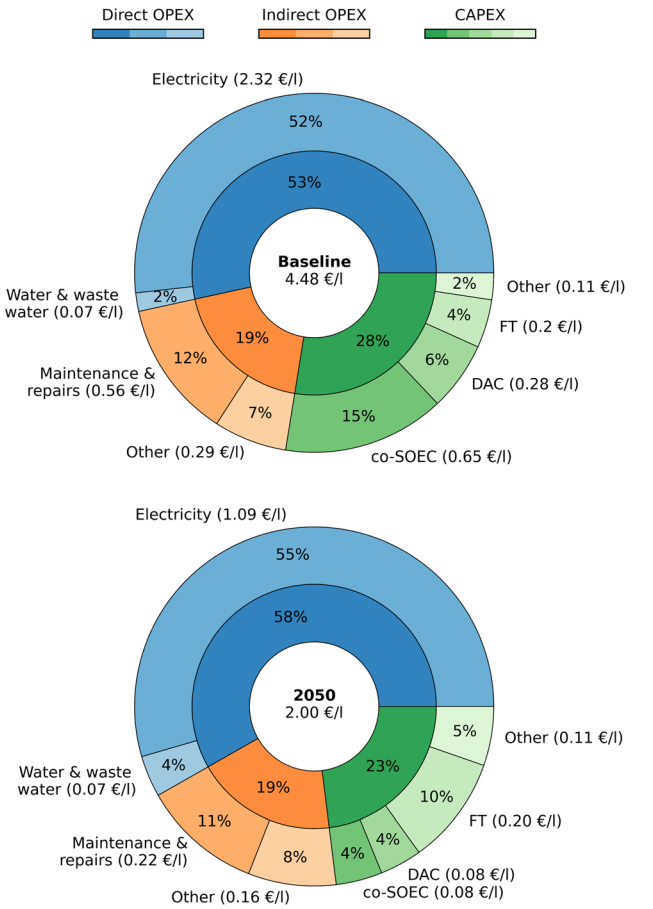

Fig. 7 Breakdown of the cost components of the NPC for the baseline scenario and the 2050 scenario (figures do not add up precisely due to rounding).

Open Access Article. Published on 15 2024. Downloaded on 16.08.24 13:28:08.
This article is licensed under a Creative Commons Attribution 3.0 Unported Licence.

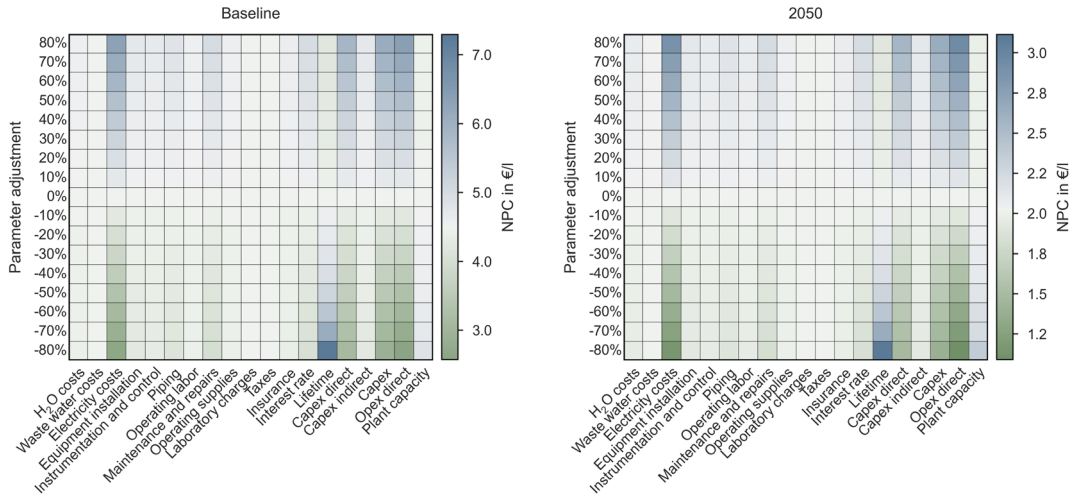

Fig. 8 Sensitivity of the NPC to a variation of ±80% in commodity costs, CAPEX factors and OPEX factors based on the assumptions described in Section 2.5.

This is in line with the interrelation between the electrical efficiency and the resulting NPC shown in Fig. 4. As the electrical efficiency mainly affects the direct OPEX *via* the required electrical energy. It further supports the approach to perform the process optimization based on a maximization of the electrical efficiency instead of a minimisation of the NPC which are underlying a higher degree of uncertainty due to the broad range in the specific cost assumptions.

For the CAPEX-related components, the Fischer–Tropsch reactor is predominant and exceeds the costs of further core components like the co-SOEC and the DAC. The major reason is provided in Section 3.1. As part of the process internal recirculation, the flow rates to be handled by the FT reactor are greater than those of the co-SOEC and DAC and therefore require larger dimensions, resulting in a higher capital cost.

A comparison with the specific production costs of centralised plants based on current literature shows higher production costs for the baseline scenario, mainly due to the efficiency loss induced by the product-related constraints and higher CAPEX. The difference in CAPEX is subject to the high capital costs of the special core components due to the early stage of development. When adjusted for differences in electricity cost assumptions, the NPC of the 2050 projection are in the same order of magnitude as current projections for centralised plants in literature.[20] Here, the advantages of an economy of scale for centralised plants with high production capacity are offset by the advantages of the assumed lower indirect costs for the decentralised modular plants. However, the NPC are still slightly higher due to the difference in efficiency of around 10% caused by the increased product composition requirements considered in this study.

The NPC's sensitivity analysis to an adjustment in cost-related assumptions is shown in Fig. 8. In line with the aforementioned observations, the variation in electricity costs has the most relevant impact on the NPC. A prolongation of the plant lifetime or a decrease of the interest rate shows only minor potential for an additional reduction of the NPC, due to the cost structure which is mainly driven by OPEX. At this point it is important to highlight the relevance of the system boundaries. In our study, electrical energy is considered as an external commodity that is generated outside the system boundaries and procured, for example, *via* an electricity grid. It can therefore be treated as an operating cost. If it is necessary to invest in a dedicated energy supply, *e.g.* if there is no grid with a sufficient share of renewable energy at the location of operation, the system boundary should be extended to encompass all relevant equipment for the required energy supply. In this case, the resulting electricity supply cost is derived from the equipment costs rather than the operation costs and would thus be directly affected by the interest rate, significantly increasing the sensitivity of the NPC to this parameter. However, the evaluation and optimisation of the upstream process chain to further cover a stable decentralised supply of renewable electricity is beyond the scope of this work.

There are no further significant impacts of single cost-components on the NPC in addition to the electricity costs. Additional major effects are exhibited only by a specific variation of higher-level cost groups, such as a general increase in direct CAPEX.

A consideration of the uncertainties underlying the assumed cost assumptions leads to the NPC bandwidths shown in Fig. 9. Based on the uncertainty ranges presented in Table 4, the baseline scenario exhibits a significant variation, resulting in

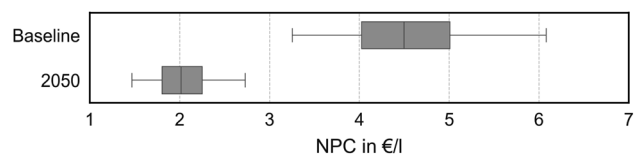

Fig. 9 Uncertainty assessment of the NPC. The box shows the interquartile range – the middle 50%. The whiskers define the 95% confidence interval.

 This journal is © The Royal Society of Chemistry 2024

Open Access Article. Published on 15 2024. Downloaded on 16.08.24 13:28:08.
This article is licensed under a Creative Commons Attribution 3.0 Unported Licence.

a wide range of estimates for the 95% confidence interval, from approximately 3.20 € per l to 6.15 € per l. The interquartile range, which includes the middle 50% of the results, is about 4.00 € per l to 5.00 € per l. With a span between approximately 1.50 € per l and 2.75 € per l for the 95% confidence interval, the costs of the 2050 scenario is considerably lower. The interquartile range is between around 1.85 € per l and 2.25 € per l. Because of the similar cost structures in both the baseline and 2050 scenarios, the relative spread of cost ranges is similar in both cases.

4 Conclusions and outlook

This study demonstrates the importance of product composition constraints on the cost of decentralised production of sustainable aviation fuel using Fischer–Tropsch synthesis as part of an electrically driven process. Compared to the efficiencies in the current literature, a process constrained in its product composition based on the assumptions made in this study faces an absolute efficiency loss of about 10% if the by-products cannot be used. For the electrical plant efficiencies, maximum values of around 35% are achievable. The restriction on the maximum proportion of product fractions below the kerosene range is particularly important here and is the main reason for the reduction in efficiency. This has a direct impact on the net production costs of kerosene, which is directly related to the electrical efficiency of the plant. At over 50%, electricity costs represent the largest share of product costs in both the baseline scenario and the 2050 projection.

This study shows that, under the assumptions made, in the long term, there is no significant difference in efficiency and production costs between the small modular units assessed in this study and large centralised plants as found in the current literature. The cost advantages of large-scale plants due to economy of scale are offset by the lower indirect costs of small modular plants, *e.g.* due to unnecessary service buildings and ease of plant operation. Net production costs of kerosene are estimated with high probability to be between around 3.20 € per l to 6.15 € per l in the baseline scenario and around 1.50 € per l and 2.75 € per l in 2050 under the assumptions made.

For this study, an open-source Python-based process modelling framework and a generic method chain were developed that can be flexibly used for other process setups. It is successfully applied to provide comprehensive insights into process interrelationships, achievable plant efficiencies, net production costs of kerosene and underlying key operating parameters for a modular power-to-liquid process unit of low complexity, taking into account various constraints. For the process setup considered in this study, the Fischer–Tropsch reaction temperature is generally identified as the most decisive operation parameter throughout the process, while the operating temperatures of the hot trap and cold trap, where the gaseous and liquid fractions are separated, have the greatest influence on the kerosene fraction of the final product composition.

This study shows that additional work is needed to consider product composition requirements to meet fuel standards in order to better understand the potential future systemic role of decentralised production of certified products. Future studies should therefore refine the product-related constraints, as these have a significant impact on the required plant complexity, plant efficiency and production costs, and thus on possible strategies for technology implementation in the energy system.

An additional focus should be on the evaluation of decentralised supply strategies for the required feedstocks, in particular electrical energy. Where a supply *via* the electricity grid is not technically or environmentally feasible, a required decentralised supply of renewable energy may increase electricity costs and material demand and have an impact on economic or environmental competitiveness with other technologies or supply strategies. Such studies could also take into account current regulations regarding the certification of a sustainable product. This is particularly relevant for issues of current interest such as the required additionality of renewable energy capacity or the temporal correlation of renewable energy supply and electricity consumption as defined by the delegated regulation of the European Commission[11] for the production of certified sustainable fuels.

Author contributions

A. Meurer: conceptualization, data curation, formal analysis, investigation, methodology, software, validation, visualization, writing – original draft, writing – review & editing; P. Jochem: supervision, writing – review & editing; J. Kern: funding acquisition, project administration, supervision, writing – review & editing.

Conflicts of interest

There are no conflicts to declare.

Acknowledgements

We acknowledge the Deutsche Gesellschaft für Internationale Zusammenarbeit (GIZ) for the funding via the project Klimaneutrale Alternative Kraftstoffe (ProQR) within the IKI framework of the German Federal Ministry for the Environment, Nature Conservation and Nuclear Safety. We further acknowledge the project SYSTÖK, funded by the German Aerospace Center (DLR), for financial support.

Notes and references

1 *United Nations Framework Convention on Climate Change, Conference of the Parties, Adoption of the Paris Agreement*, Dec. 12, 2015, U.N. Doc. FCCC/CP/2015/L.9/Rev/1, 2015.
2 D. S. Lee, D. W. Fahey, A. Skowron, M. R. Allen, U. Burkhardt, Q. Chen, S. J. Doherty, S. Freeman, P. M. Forster, J. Fuglestvedt, A. Gettelman, R. R. de Leon, L. L. Lim, M. T. Lund, R. J. Millar, B. Owen, J. E. Penner, G. Pitari, M. J. Prather, R. Sausen and L. J. Wilcox, *Atmos. Environ.*, 2021, **244**, 117834, DOI: **10.1016/j.atmosenv.2020.117834**.

Open Access Article. Published on 15 2024. Downloaded on 16.08.24 13:28:08.
This article is licensed under a Creative Commons Attribution 3.0 Unported Licence.

3 *International Council on Clean Transportation (ICCT), Vision 2050 Aligning Aviation with the Paris Agreement*, 2012.
4 H. Dalkmann and C. Brannigan, *Transport and Climate Change. Module 5e. Sustainable Transport: A Sourcebook for Policy-Makers in Developing Cities*, 2007.
5 Air Transport Action Group (ATAG), Balancing Growth in Connectivity with a Comprehensive Global Air Transport Esponse to the Climate Emergency: a Vision of Net-Zero Aviation by Mid-century, *Waypoint 2050*, 2021.
6 C. Frömming, M. Ponater, K. Dahlmann, V. Grewe, D. S. Lee and R. Sausen, *J. Geophys. Res.: Atmos.*, 2012, **117**, D19104, DOI: **10.1029/2012JD018204**.
7 German Aerospace Center (DLR), Towards Zero-Emission Aviation: How DLR's Aviation Research Strategy Supports the European, *Green Deal 2050*, 2021.
8 International Civil Aviation Organization (ICAO), *2022 Environmental Report: Innovation for a Green Transition*, 2023.
9 Council of the European Union, *Interinstitutional File: 2021/0205(COD): 9805/22*, 2022, **https://data.consilium.europa.eu/doc/document/ST-9805-2022-INIT/en/pdf**.
10 *Communication from the Commission to the European Parliament, the Council, the European Economic and Social Committee and the Committee of the Regions: COM(2021) 550 final*, ed. E. Union: European Commission, 14, 2021.
11 European Commission, *Delegated Regulation on Union Methodology for RFNBOs: C(2023) 1087 Final*, 2023, **https://energy.ec.europa.eu/system/files/2023-02/C_2023_1087_1_EN_ACT_part1_v8.pdf**.
12 European Commission, *Directive (EU) 2018/2001 of the European Parliament and of the Council of 11 December 2018 on the promotion of the use of energy from renewable sources (recast) (Text with EEA relevance.): PE/48/2018/REV/1*, 2018.
13 European Commission, Joint Research Centre, O. Hurtig, N. Scarlat, V. Motola, M. Buffi, A. Georgakaki, S. Letout, A. Mountraki and G. Joanny, *Clean Energy Technology Observatory, Renewable Fuels of Non-biological Origin in the European Union : Status Report on Technology Development, Trends, Value Chains and Markets : 2022*, Publications Office of the European Union, 2022.
14 A. C. Ince, C. O. Colpan, A. Hagen and M. F. Serincan, *Fuel*, 2021, **304**, 121354, DOI: **10.1016/J.FUEL.2021.121354**.
15 D. H. König, M. Freiberg, R.-U. Dietrich and A. Wörner, *Fuel*, 2015, **159**, 289–297, DOI: **10.1016/j.fuel.2015.06.085**.
16 F. G. Albrecht, D. H. König, N. Baucks and R.-U. Dietrich, *Fuel*, 2017, **194**, 511–526, DOI: **10.1016/j.fuel.2016.12.003**.
17 R. Peters, N. Wegener, R. C. Samsun, F. Schorn, J. Riese, M. Grünewald and D. A. Stolten, *Processes*, 2022, 699, DOI: **10.3390/pr10040699**.
18 G. Herz, E. Reichelt and M. Jahn, *Appl. Energy*, 2018, **215**, 309–320, DOI: **10.1016/j.apenergy.2018.02.007**.
19 S. Adelung, *J. CO2 Util.*, 2022, **65**, 102171, DOI: **10.1016/j.jcou.2022.102171**.
20 P. Schmidt, V. Batteiger, A. Roth, W. Weindorf and T. Raksha, *Chem. Ing. Tech.*, 2018, **90**, 127–140, DOI: **10.1002/cite.201700129**.
21 M. Loewert, J. Hoffmann, P. Piermartini, M. Selinsek, R. Dittmeyer and P. Pfeifer, *Chem. Eng. Technol.*, 2019, **42**, 2202–2214, DOI: **10.1002/ceat.201900136**.
22 C. Kjelgaard, *Standard for 100 Percent Drop-In SAF Likely Two Years Away, Air Transport News: Aviation International News*, **https://www.ainonline.com/aviation-news/air-transport/2022-07-18/standard-100-percent-drop-saf-likely-two-years-away**, accessed 01.09.2023.
23 S. Kramer, G. Andac, J. Heyne, J. Ellsworth, P. Herzig and K. C. Lewis, *Front. Energy Res.*, 2022, **9**, 782823, DOI: **10.3389/fenrg.2021.782823**.
24 A. Meurer and J. Kern, *Energies*, 2021, **14**(7), 1836, DOI: **10.3390/en14071836**.
25 Norsk e-fuel AS, Coming Soon: Green Jet-Fuel From Mosjøen, Norway, 28.02.2022, **https://f.hubspotusercontent-eu1.net/hubfs/25457266/NEF%20Press%20Release_final_CD_ENG.pdf**, accessed 01.09.2023.
26 H. Kirsch, L. Brübach, M. Loewert, M. Riedinger, A. Gräfenhahn, T. Böltken, M. Klumpp, P. Pfeifer and R. Dittmeyer, *Chem. Ing. Tech.*, 2020, **92**(1–2), 91–99, DOI: **10.1002/cite.201900120**.
27 atmosfair, *atmosfair FairFuel: Power-to-Liquid Kerosene Production*, 2021, **https://fairfuel.atmosfair.de/wp-content/uploads/2021/10/Short-description_atmosfair_E-Kerosene-plant_EN_092021.pdf**, accessed 01.09.2023.
28 A. de Klerk, *Green Chem.*, 2008, **10**, 1249–1279, DOI: **10.1039/B813233J**.
29 M. Loewert, V. Z. Francesconi, L. T. Brübach and P. Pfeifer, *Chem. Eng. J.*, 2020, **402**, 126032, DOI: **10.1016/j.cej.2020.126032**.
30 H. Kirsch, N. Lochmahr, C. Staudt, P. Pfeifer and R. Dittmeyer, *Chem. Eng. J.*, 2020, **393**(124553), DOI: **10.1016/j.cej.2020.124553**.
31 D.-Y. Peng and D. B. Robinson, *Ind. Eng. Chem. Fundam.*, 1976, **15**, 59–64, DOI: **10.1021/i160057a011**.
32 C. L. Yaws, Physical Properties – Organic Compounds, *The Yaws Handbook of Physical Properties for Hydrocarbons and Chemicals*, ed. C. L. Yaws, Gulf Professional Publishing, 2015, DOI: **10.1016/B978-0-12-800834-8.00001-3**.
33 C. L. Yaws, *Critical Properties and Acentric Factor – Organic Compounds, Thermophysical Properties of Chemicals and Hydrocarbons*, Gulf Publishing Company, 2014, 2nd edn, DOI: **10.1016/B978-0-323-28659-6.00001-X**.
34 C. L. Yaws and M. A. Satyro, Vapor Pressure – Organic Compounds, *The Yaws Handbook of Vapor Pressure*, Gulf Professional Publishing, 2015, DOI: **10.1016/B978-0-12-802999-2.00001-5**.
35 M. Fasihi, O. Efimova and C. Breyer, *J. Cleaner Prod.*, 2019, **224**, 957–980, DOI: **10.1016/j.jclepro.2019.03.086**.
36 Sunfire GmbH, *Sunfire-SynLink SOEC - Technical Data*, 2021**https://www.sunfire.de/files/sunfire/images/content/Sunfire.de%20(neu)/Sunfire-Factsheet-SynLink-SOEC-20210303.pdf**, accessed 01.09.2023.
37 T. Smolinka, N. Wiebe, P. Sterchele and A. Palzer, *Studie IndWEDe: Industrialisierung der Wasserelektrolyse in Deutschland: Chancen und Herausforderungen für*

Open Access Article. Published on 15 2024. Downloaded on 16.08.24 13:28:08.
This article is licensed under a Creative Commons Attribution 3.0 Unported Licence.

nachhaltigen Wasserstoff für Verkehr, Strom und Wärme, NOW GmbH, 2018.

38 C. Sun, Direct syngas-to-fuel: integration of Fischer-Tropsch synthesis and hydrocracking in micro-structured reactors, PhD Thesis, Karlsruher Institut für Technologie, Karlsruhe, 2017.

39 S.-H. Kwack, M.-J. Park, J. W. Bae, K.-S. Ha and K.-W. Jun, Development of a kinetic model of the Fischer–Tropsch synthesis reaction with a cobalt-based catalyst, *React. Kinet., Mech. Catal.*, 2011, **104**, 483–502, DOI: **10.1007/s11144-011-0369-1**.

40 A. de Klerk, *Energy Environ. Sci.*, 2011, **4**, 1177–1205, DOI: **10.1039/C0EE00692K**.

41 A. de Klerk, *Fischer-Tropsch Refining*, Wiley-VCH Verlag GmbH & Co. KGaA, 2011.

42 L. A. Pellegrini, S. Gamba, V. Calemma and S. Bonomi, *Chem. Eng. Sci.*, 2008, **63**, 4285–4291, DOI: **10.1016/j.ces.2008.06.002**.

43 D. Selvatico, A. Lanzini and M. Santarelli, *Fuel*, 2016, **186**, 544–560, DOI: **10.1016/j.fuel.2016.08.093**.

44 S. Sircar and T. C. Golden, *Sep. Sci. Technol.*, 2000, **35**, 667–687, DOI: **10.1081/SS-100100183**.

45 C. L. Tucker, M. Claeys and E. van Steen, *Catal. Sci. Technol.*, 2020, **10**, 7056–7066, DOI: **10.1039/D0CY00929F**.

46 *Chevron, Alternative Jet Fuels – A Supplement to Chevron's Aviation Fuels Technical Review*, 2006, **https://skybrary.aero/sites/default/files/bookshelf/2479.pdf**, accessed 01.09.2023.

47 ASTM International, ASTM D1655-22, Standard Specification for Aviation Turbine Fuels, 2022.

48 ASTM International, ASTM D7566-18, Standard Specification for Aviation Turbine Fuel Containing Synthesized Hydrocarbons, 2018.

49 C. Voigt, J. Kleine, D. Sauer, R. H. Moore, T. Bräuer, P. Le Clercq, S. Kaufmann, M. Scheibe, T. Jurkat-Witschas, M. Aigner, U. Bauder, Y. Boose, S. Borrmann, E. Crosbie, G. S. Diskin, J. DiGangi, V. Hahn, C. Heckl, F. Huber, J. B. Nowak, M. Rapp, B. Rauch, C. Robinson, T. Schripp, M. Shook, E. Winstead, L. Ziemba, H. Schlager and B. E. Anderson, *Commun. Earth Environ.*, 2021, **2**, 114, DOI: **10.1038/s43247-021-00174-y**.

50 M. D. McKay, R. J. Beckman and W. J. Conover, *Technometrics*, 1979, 239–245.

51 D. Wang, D. Tan and L. Liu, *Soft Comput.*, 2018, **22**, 387–408, DOI: **10.1007/s00500-016-2474-6**.

52 J. S. Arora, O. A. Elwakeil and A. I. Chahande, *Structural Optimization*, 1995, 137–159.

53 A. P. Piotrowski, J. J. Napiorkowski and A. E. Piotrowska, *Swarm Evol. Comput.*, 2020, **58**(100718), DOI: **10.1016/j.swevo.2020.100718**.

54 M. S. Peters, K. D. Timmerhaus and R. E. West, *Plant Design and Economics for Chemical Engineers: 5th edn*, McGraw-Hill Higher Education, New York, USA, 5th edn, 2004.

55 Institut der Deutschen Wirtschaft Köln e.V., *IW-Trends 2/2019: Industrielle Arbeitskosten im internationalen Vergleich*, **https://www.iwkoeln.de/fileadmin/user_upload/Studien/IW-Trends/PDF/2019/IW-Trends_2019-02-05_Industrielle_Arbeitskosten.pdf**, accessed 01.09.2023.

56 A. Meurer, P. Jochem and J. Kern, Decentralised Production of E-Fuels for Aviation: Calculation Results, *Zenodo*, 2023, DOI: **10.5281/zenodo.8260478**.

57 K. Atsonios, J. Li and V. J. Inglezakis, *Energy*, 2023, **278**, 127868, DOI: **10.1016/j.energy.2023.127868**.